Effect of Mass Transfer on Flow Across a Staggered Tube Bundle

S. Aly† and J. Cunningham‡

Over a range of Reynolds numbers from $0{\cdot}6 \times 10^5$ to $1{\cdot}75 \times 10^5$ tests were made on a seven rows deep tube bank. These tests were made using a specially instrumented porous cylinder which could be located in any position within the bank. Mass transfer through the porous surface simulating the condensation process in a surface condenser, was applied, and its effect on local parameters investigated. The distribution of static pressure and skin friction was determined around tubes in different rows in the bank. From these measurements, the pressure drag and friction drag were estimated. The total pressure drop across the bank was also measured.

Results showed that, for typical steam condenser loadings, the contribution of the pressure drag to the total drag does not change appreciably with suction. However, the skin friction contribution does change considerably with suction.

NOTATION

A	tunnel cross-sectional area
CQ	suction to main flow flux ratio
C_f	shear drag
CP	pressure coefficient
D	cylinder outside diameter
H	height of working section
K_f	local friction factor
KD	pressure drag
KS	particle diameter of porous material
L	longitudinal pitch
N	number of tubes per row
P	normal pressure
Re	Reynolds number
T	transverse pitch
U	flow velocity
τ	skin friction
ρ	density of main flow fluid

Subscripts

θ	angle measured from fsp
max	based on minimum free area
a	approach
w	wake
∞	undisturbed stream

INTRODUCTION

In a shell and tube heat exchanger, e.g., a steam surface condenser, the velocity of the shell-side fluid relative to the tubes varies in magnitude and direction throughout the bundle. In a baffled exchanger, the flow between the baffles approaches pure cross-flow, depending on the baffle spacing. The presence of the tubes presents a restriction to fluid flow.

The important pressure drop in a steam condenser is between the inlet exhaust casing and the non-condensable gas extraction section. A large pressure drop in an exchanger is highly undesirable due to its effect on exchanger performance. For example, in a steam condenser, pressure drop affects the temperature of heat rejection, which is a major factor in the overall efficiency of power plant.

Drummond (**1**) and Morsy (**2**) showed that condensation could modify tube bundle pressure loss by reducing the pressure drag in surface condensers.

This article presents results on the detailed flow mechanism in a tube bundle using a newly developed instrument for measuring skin friction on cylindrical surfaces.

EXPERIMENTAL APPARATUS

The experimental rig consisted of a seven rows deep tube bank, with three cylinders per row, located in a wind tunnel. The local flow parameters were obtained on a specially instrumented cylinder made from sintered bronze with a roughness parameter of $KS/D = 53 \times 10^{-5}$, where KS was the average diameter of the spherical bronze particles. The cylinders were mounted vertically in the working section and the instrumented one, which could be located in any row in the bank, could be rotated about its longitudinal axis from outside the tunnel. Each tube had an outside diameter of 76·2 mm and a total length of 381 mm. All tubes, except the instrumented tube, were made of aluminium. The dimensionless transverse pitch, T, and the longitudinal pitch, L, were equal and were chosen to be 1·5 times the tubes' outside diameter. The working section was 381 × 343 × 1220 mm.

The test cylinder was connected to an extraction system which could be used to suck air through the porous wall of the cylinder. The thickest available wall for the porous tube was used to provide for almost uniform suction around the cylinder circumference. Pressures inside and outside the cylinder were monitored and from these the suction rate could be calculated.

Static pressure and skin friction were measured simultaneously using the instrumented cylinder. At the mid-height of this cylinder, a newly developed skin friction gauge was mounted. A detailed description of the gauge, its installation and operation is given by Cunningham

† Lecturer, Reactors Department, Atomic Energy Establishment, Cairo, Egypt, formerly of the University of Glasgow.
‡ Lecturer, Department of Mechanical Engineering, University of Glasgow, Glasgow, Scotland.
Received 15 February 1979 and accepted for publication 12 October 1979.

0142/727X/79/1200-0169$02.00

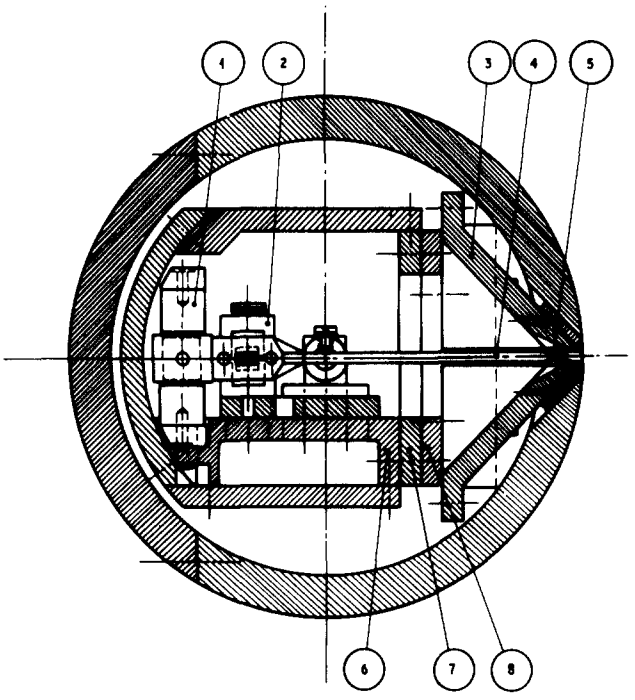

Fig. 1. Schematic diagram of the assembled device. (1) electromagnetic coils; (2) photoelectric system; (3) supporting frame; (4) movable assembly; (5) side spacers; (6) adjustable carrier; (7) & (8) sliding adjustable frames

and Aly (**3**). Briefly, the gauge was a self-centering null-seeking force balance. The balance consisted of a vane of nonmagnetic material mounted on a pair of frictionless cross-spring flexural pivots. One end of the vane replaced an area on the outside surface of the cylinder (Fig. 1). This end, the drag piece, was exposed to the main flow while a restoring force was applied to the other end of the vane by means of a transducer and control system, Macvean and Aly (**4**). Since there was a considerable pressure gradient around the cylinder, the shear force measurements obtained directly from the gauge had to be corrected for the buoyancy effect caused by the difference in pressures between the leading and trailing edges of the drag piece. This amounted to about 3 per cent of the measured shear forces.

Due to the presence of heating coils upstream of the bank, which were to be used in later experiments, it was found that the turbulence level of the air stream incident to the first row of the bank was increased to a value of 6 per cent compared to the undisturbed turbulence level of 1·2 per cent.

Because of the limited capacity of the fan, the upper limit of the Reynolds number which could be reached, based on the undisturbed flow velocity, was about $0{\cdot}7 \times 10^5$. It should be noted that this is an order of magnitude less than the Reynolds numbers encountered in normal power station condensers. Measurements were taken in five degree steps from the front stagnation point (fsp) to the rear of the cylinder.

The total pressure drop over the bank, with varying depth, was obtained by measuring the pressure difference between two stations. The first was more than 1·5 D upstream of the bank, before the effect of blockage started, Kestin and Wood (**5**). The second was more than 2 L downstream of the last row, where pressure recovery was complete, Pearce (**6**).

PRESENTATION OF RESULTS

The data for shear force presented here are uncorrected for the clearance gap effect. This results in forces being 3 per cent too high using the method of Depooter, *et al.* (**7**) or 8 per cent too high using the method of Hoerner (**8**).

The dimensionless presentation of normal pressure distribution around the tubes in different rows in the bank is not shown in the same way as for single cylinders, since there was no undisturbed flow upstream of each row in the bank. Achenbach (**9**) defined a hypothetical dynamic pressure based on a maximum velocity, U_{max}, calculated from the mass flow through the smallest cross-section. As a result the local pressure coefficient at an angle θ measured from the fsp was

$$CP_\theta = 1 - \frac{P_{\theta=0} - P_\theta}{\frac{1}{2}\rho U_{max}^2} \tag{1}$$

This choice of reference velocity, however, allows no comparison between local parameters in various rows in the bank since velocity variations through the bank are not taken into account.

The method used in this paper is to express CP_θ as

$$CP_\theta = \frac{P_\theta - P_w}{\frac{1}{2}\rho U_a^2} \tag{2}$$

where P_w is the wake pressure in the preceding row, measured at the rear of the cylinders in that row. U_a is the approach velocity to the row under consideration, and so the value of CP_θ is always unity at $\theta = 0$.

For the first row in the bank, the approach velocity was that in the main stream corrected for the blockage effect, Allen and Vincenti (**10**).

Based on these estimated approach velocities, the shear stress is presented in the following dimensionless form

$$K_f = \tau/\tfrac{1}{2}\rho U_a^2 \tag{3}$$

The contribution of the pressure drag to the total drag was obtained by integrating the normal pressure

$$KD = \int_0^\pi CP_\theta \,.\, \cos\theta \,.\, d\theta \tag{4}$$

The contribution of the skin friction to the total drag was obtained in a similar manner

$$C_f = \int_0^\pi K_f \,.\, \sin\theta \,.\, d\theta \tag{5}$$

For the mass extraction tests, the normal velocity, V_0, into the surface of the porous cylinder was obtained from the pressure drop across the wall, and the values of material porosity recommended by the tube manufacturer. These values were checked against a calibrated rotameter and the agreement was found to be within ± 5 per cent. Results of the mass extraction tests were correlated against the dimensionless suction parameter $CQ\sqrt{Re}$, where CQ is the ratio of the suction velocity, calculated from the mass flow through the porous surface, to the approach velocity.

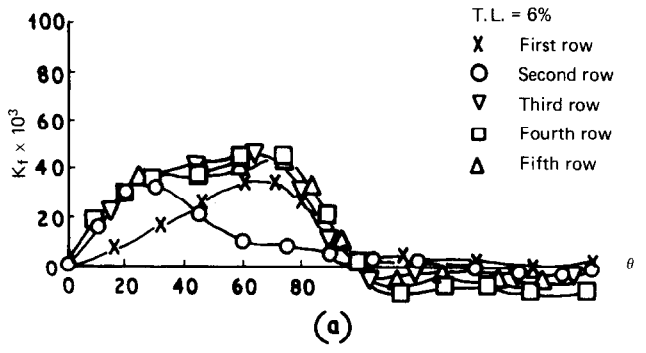

Fig. 2(*a*). Skin friction distribution in the bank $Re_\infty = 0{\cdot}27 \times 10^5$

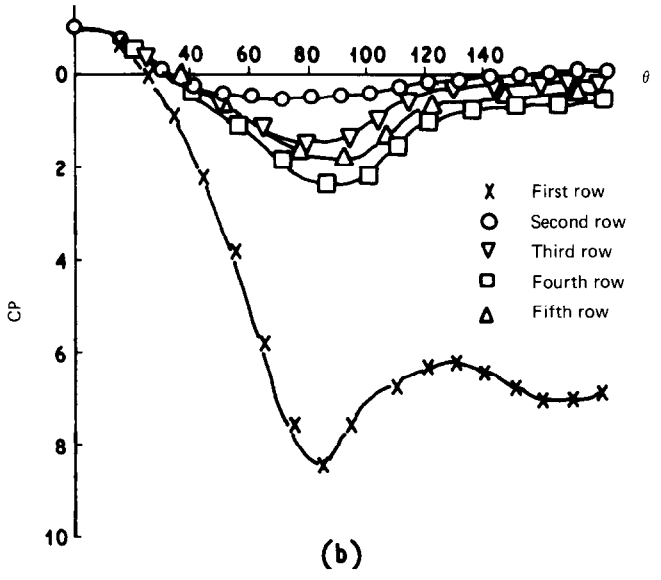

Fig. 2(*b*). Pressure coefficient distribution in the bank $Re_\infty = 0{\cdot}27 \times 10^5$

RESULTS

A sample of the data obtained for the no-suction tests is presented in Figs. 2–4 for differing values of Reynolds number. Figures 2*a*, 3*a*, and 4*a* show the variation in skin friction for different rows in the bank, and Figs. 2*b*, 3*b*, and 4*b* demonstrate the corresponding variations in pressure distributions in these rows. It is apparent that the largest pressure variation occurs in the first row of the bank; this is mainly due to the blockage effect. As the blockage ratio increases, the flow around the tube outside the boundary layer accelerates and the pressure distribution is changed accordingly. It is apparent that flow around cylinders in the first row is similar to that around single sylinders in cross-flow under similar blockage restrictions. Figure 2*b* shows the effect the second row has on the pressure distribution round tubes in the first row.

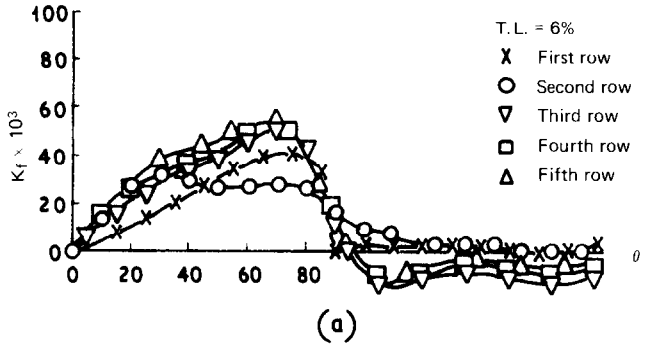

Fig. 3(*a*). Skin friction distribution in the bank $Re_\infty = 0{\cdot}47 \times 10^5$

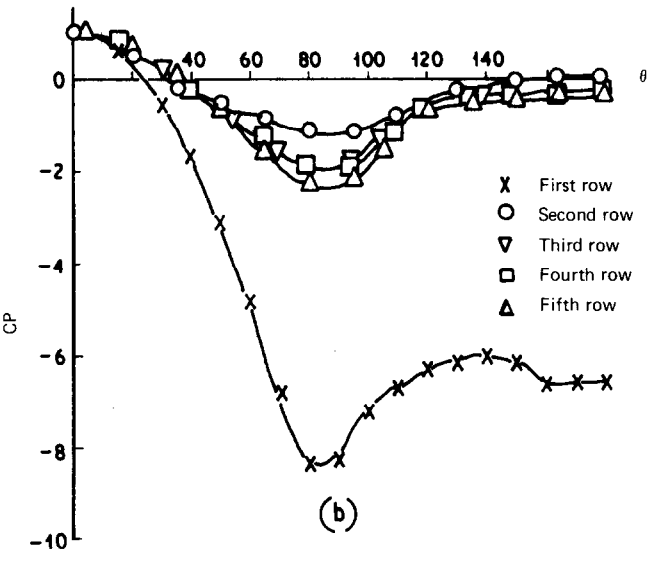

Fig. 3(*b*). Pressure coefficient distribution in the bank $Re_\infty = 0{\cdot}47 \times 10^5$

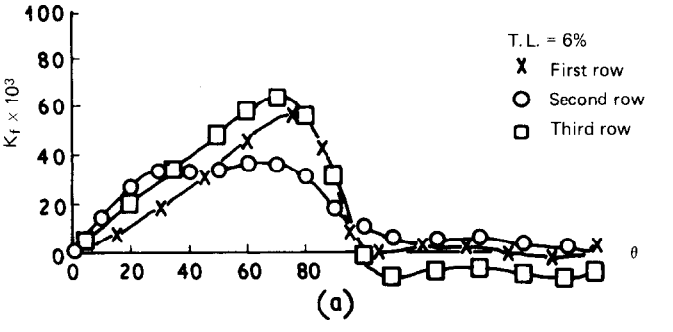

Fig. 4(*a*). Skin friction distribution in the bank $Re_\infty = 0{\cdot}7 \times 10^5$

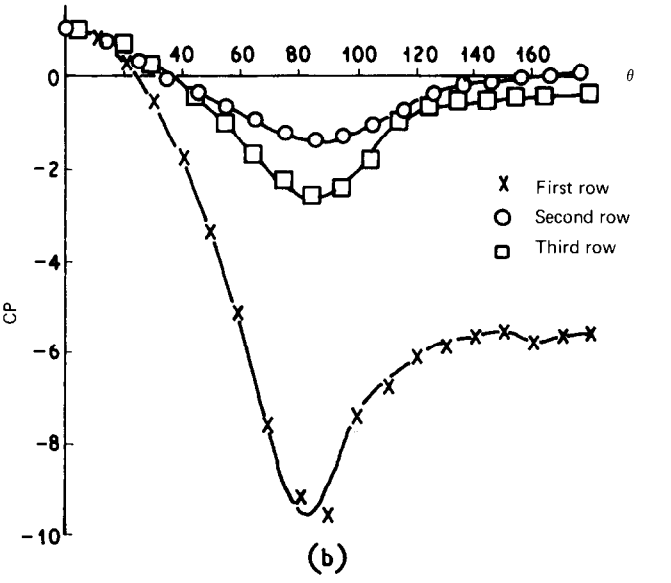

Fig. 4(*b*). Pressure coefficient distribution in the bank $Re_\infty = 0{\cdot}7 \times 10^5$

Instead of a constant pressure on the rear of the first row, the pressure starts to drop gradually after $\theta = 130°$ till it reaches the rear stagnation point. With increasing Reynolds number, Figs. 3*b* and 4*b*, the back pressure flattens out. This implies that, as the Reynolds number increases, the wake width reduces, and so the interference of the successive row on the preceding one reduces.

From Fig. 2*b* it can be seen that the point of minimum pressure for all rows except the second lies between $\theta = 85°$ and 90°.

The unique characteristics of the second row are due to the fact that a tube situated in this row is subjected, in part, to the accelerated flow emerging from the first row.

As far as local parameters on the second row are concerned, it can be seen that increasing the Reynolds number displaces the point of minimum pressure from $\theta = 70°$, Fig. 2*b*, to $\theta = 85°$, Fig. 4*b*. It is obvious that the displacement of the minimum pressure point towards the rear of the cylinder with increasing Reynolds number is associated with a similar movement of the separation point towards the rear stagnation point.

The skin friction distribution around the tubes in this row is relatively flat compared to the other rows, with characteristic twin maxima at $\theta = 30°$ and $\theta \simeq 70°$.

The change in pressure drag encountered by the flow over different rows in the bank is shown in Fig. 5 along with single cylinder results for comparison. In general, pressure decreases with increasing Reynolds number. The maximum pressure drag is encountered on the first row, due to the flow acceleration and the associated severe pressure gradient, and is about five times that encountered on a single cylinder under similar undisturbed flow conditions. On the other hand, the smallest pressure drag occurs on the second row as a result of the low pressure at the rear of the cylinders in that row. It is possible that there is some pressure recovery at the rear of the second row as the flow decelerates passing over this row. The apparent steadiness of the flow after the third row can be attributed to the turbulence caused by the preceding rows increasing to some steady value at

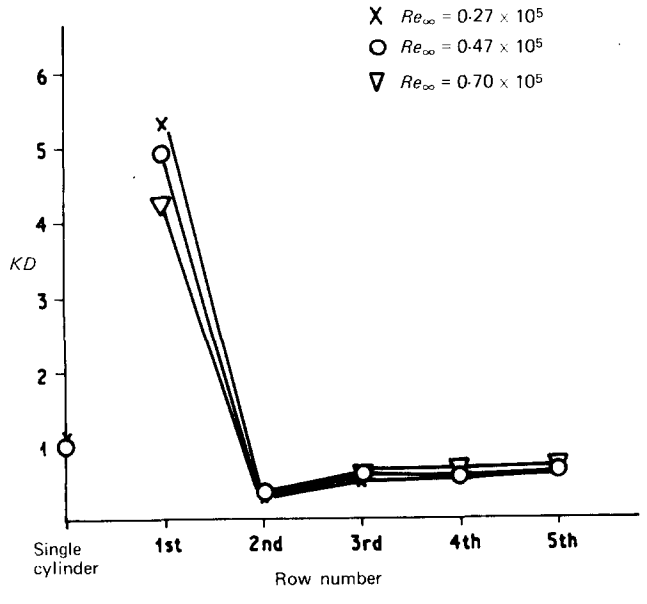

Fig. 5. Pressure drag on different rows in the bank

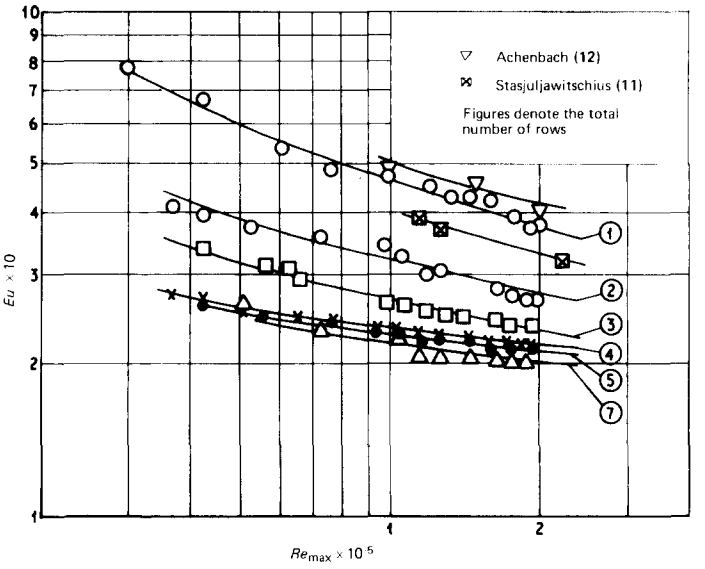

Fig. 6. Hydraulic resistance of a staggered bank referred to one row

this section of the bank. As a result, there is no further gain in pressure and similar characteristics are obtained for the fourth and fifth rows in the bank.

The total pressure drop over banks of varying depth was also measured. Figure 6 shows the variation in Euler number, which is four times the drag coefficient, referred to one row as a function of Reynolds number based on the flow velocity in the minimum free cross-section of the bank. Data are also presented for a single row as measured by Stasjuljawitschius (**11**) for a transverse pitch of 1·5 and by Achenbach (**12**) for a transverse pitch equal to 2.

By neglecting the effect of the side walls of the working section, the percentage momentum loss for each row could be computed by integrating the local static pressure and skin friction distributions to yield the contribution of each of these to the total drag. The summation of each of these contributions should yield the total drag. Consequently, the pressure drop encountered by the flow passing over a particular row could be calculated from

$$\Delta P \,.\, A = (KD + C_f) \,.\, \tfrac{1}{2}\rho U_a^2 \,.\, D \,.\, H \,.\, N \qquad (6)$$

This expression was applied to each of the first five rows in the bank, and results correlated against Reynolds number are presented in Fig. 7. The results of Achenbach (**9**), Jakob (**13**), Grimisson (**14**) and Zukauskas (**15**) are also presented for comparison. The agreement between the integrated values and the measured total pressure drop is reasonable.

Figures 6 and 7 show that pressure drop decreases as the flow moves deeper into the bank. It should be noticed in Fig. 7 that the integrated values over the fifth row are about 20 per cent to 30 per cent higher than those calculated from the total pressure drop across the bank. This difference could be attributed to the difference in surface conditions in both cases, since the total pressure drop was measured across a smooth bank, and the integrated values were obtained on the porous cylinder. The effect of surface roughness on local values is given by Cunningham and Aly (**3**). It is noticeable that data calculated for the first row are quite high, even

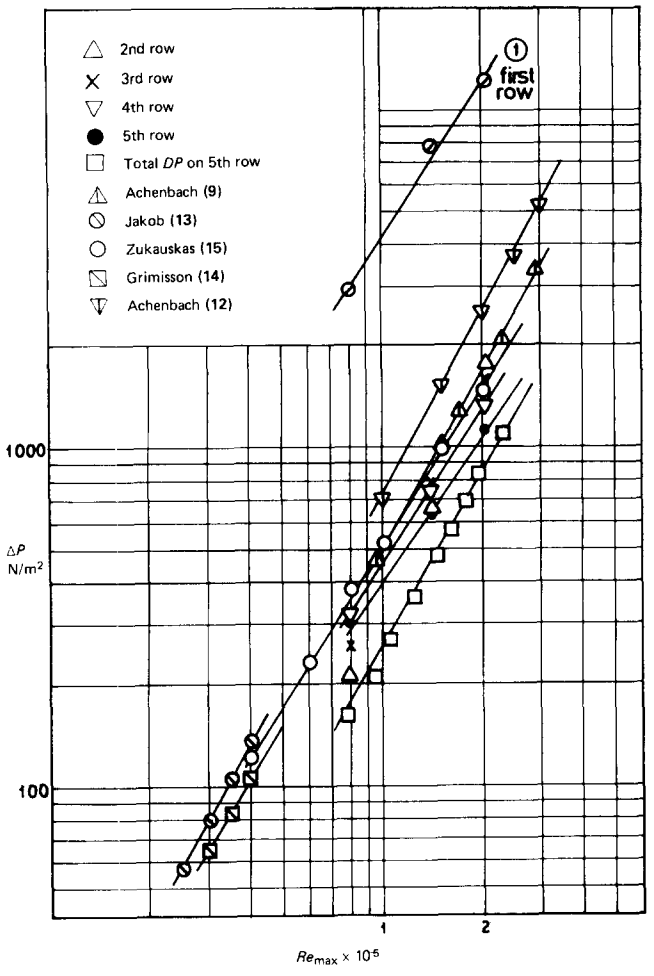

Fig. 7. Pressure drop in the bank

compared with those reported by Achenbach (9). The reason for this difference might be due to the difference in transverse pitch used in each investigation.

The present results indicate that, as would be expected, the shallower the bank, the higher the drag factor per row. Each row acts as an artificial turbulator for the succeeding one, but after a certain number of rows, depending on the bank, the flow stabilizes. For example, in the present bank stable conditions set in at about the fourth row.

The percentage contribution of the shear stress to the total drag ranged between 2 per cent and 4 per cent in the investigated flow range. These values show that although the shear stress does not significantly influence the total drag it does, however, influence the flow by affecting the position of the separation point and the width of the recirculation region, and consequently influences the pressure drag.

THE EFFECT OF SUCTION

Both Drummond (1) and Morsy (2) showed that condensation on a tube in a surface condenser could be simulated by mass extraction through a porous tube in a tube bundle.

Figures 8 and 9 show examples of the measured parameters and show the progressive effect of suction on flow across the first two rows in the bank. The suction rate investigated was chosen to cover the range normally encountered in steam surface condensers, that is, $CQ\sqrt{Re}$ from 0 to 0·8. In this range, suction (mass extraction) has a greater effect on the skin friction distribution than on the pressure distribution.

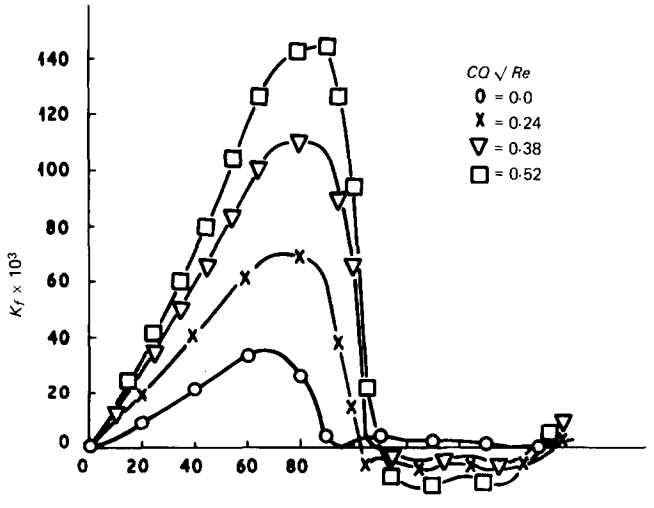

Fig. 8. Skin friction distribution with suction on the first row in the bank, $Re_\infty = 0{\cdot}6 \times 10^5$

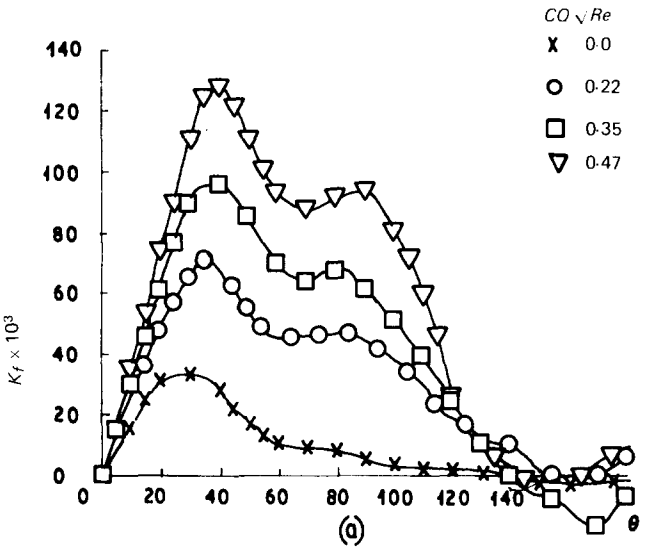

Fig. 9(*a*). Effect of suction on skin friction distribution on second row, $Re_\infty = 0{\cdot}76 \times 10^5$

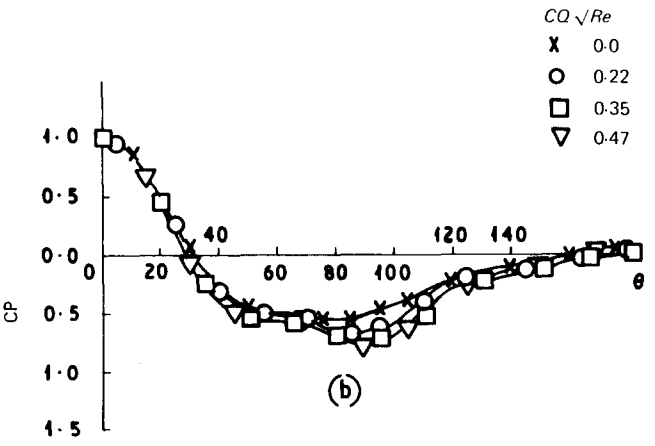

Fig. 9(*b*). Effect of suction on pressure coefficient distribution on second row, $Re_\infty = 0{\cdot}76 \times 10^5$

Figure 8 shows the variation of skin friction with suction rate in the first row of the bank. It can be seen that skin friction increases considerably with suction whereas the separation point and the point of maximum skin friction are progressively displaced towards the rear of the cylinder. The variations in pressure drag in this row were not significant, within ± 2 per cent of values without suction, Fig. 2*b*.

The effect of suction on the second row is shown in Figs. 9*a* and 9*b*. As a general characteristic of this row, the skin friction distribution has maintained its two peaks; however, these are retarded towards the rear of the cylinders.

Variations of pressure drag on the second row were slightly more than those for the first row, within $+8$ per cent to -13 per cent of values without suction.

Flow characteristics around the third to fifth rows showed the same general trend as demonstrated on the previous rows, Fig. 10. With increasing mass extraction, the shear stress increases markedly and the separation point is retarded, accompanied by small variations in pressure drag. The complete results for these rows are not presented due to limitations of space.

One of the noticeable features of the skin friction measurements is its non-zero magnitude at $\theta = 180°$.

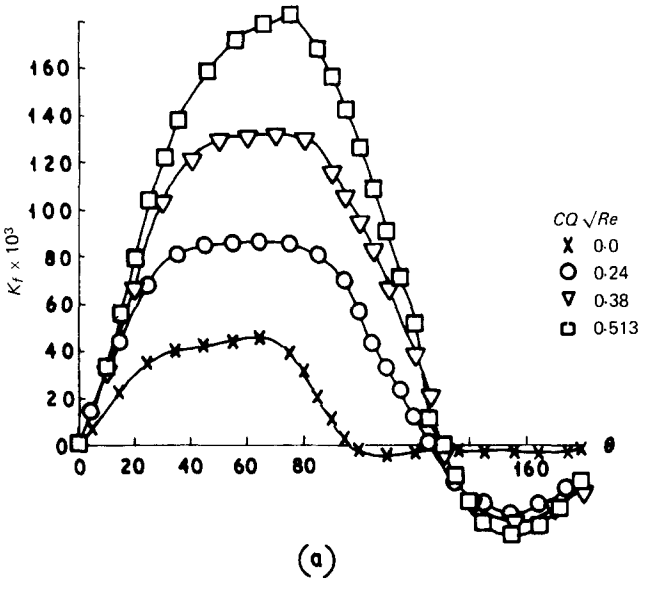

Fig. 10(*a*). Effect of suction on skin friction distribution on third row, $Re_\infty = 0{\cdot}6 \times 10^5$

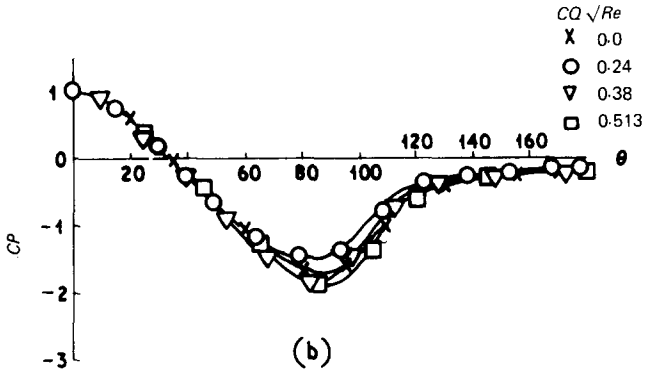

Fig. 10(*b*). Effect of suction on pressure distribution on third row, $Re_\infty = 0{\cdot}6 \times 10^5$

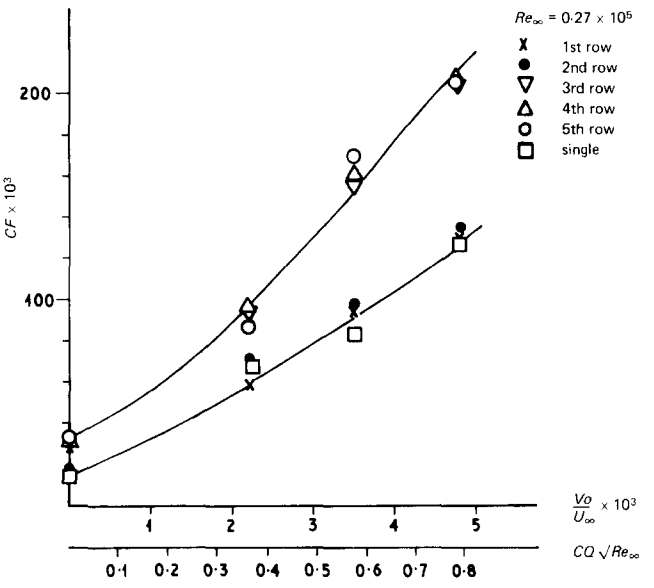

Fig. 11. Average skin friction with mass transfer on the bank at $Re_\infty = 0{\cdot}27 \times 10^5$

This should not have been the case if this point were the rear stagnation point. This can be explained, following Pankhurst and Thwaites (**16**), by assuming that the rear stagnation point was not on the surface of the cylinder itself. According to Schwabe (**17**) this free stagnation point may be unstable due to vortex shedding and the tendency for disturbances to be amplified in regions of rising pressure.

The effect of mass extraction on the skin friction contribution to the total drag was calculated from expression (5), and results are shown in Figs. 11 and 12 for two Reynolds numbers, $0{\cdot}27 \times 10^5$ and $0{\cdot}47 \times 10^5$, respectively. As the maximum suction rate only accounted for 0·2 per cent of the main flow the effect of mass extraction on main flow velocity is neglected. Single cylinder results are also included for comparison.

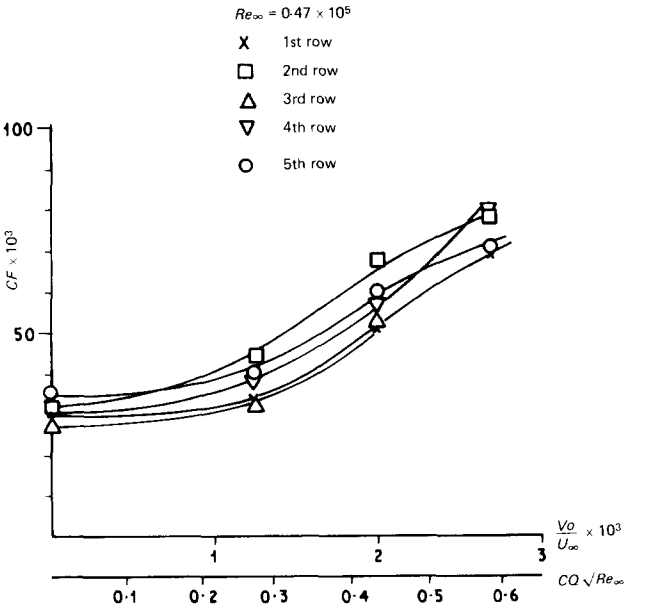

Fig. 12. Average skin friction with mass transfer on the bank at $Re_\infty = 0{\cdot}47 \times 10^5$

As would be expected, mass extraction increases the skin friction over the whole bank with differing rates for different rows. Figure 11 shows that the first and second rows together with the single cylinder had lower values compared with those for the third row onwards, at the same suction rates.

CONCLUDING REMARKS

In the present work, local values of skin friction and normal pressure were measured around cylinders in different rows in a tube bank. The results were obtained under isothermal conditions and results for nonisothermal experiments will be presented in a subsequent article.

With respect to mass extraction on flow in a tube bank, the main points could be summarized as follows.

(1) For typical steam condenser loadings, condensation, or mass extraction, might have some effect on the pressure distribution round different rows in the bank. However, the mass transfer effect on the contribution of the pressure drag to the total drag is not significant.
(2) The skin friction is highly sensitive to mass extraction and increases with increasing suction.
(3) The correlation between skin friction and the normal pressure distribution for those cases where suction was applied is much more complex than that without suction. More data are required to produce such a correlation.

REFERENCES

(1) DRUMMOND, C. 'Pressure recovery in condensation processes', *Ph.D. Thesis* 1966, Heriot-Watt Univ., Scotland.
(2) MORSY, M. 'Skin friction and form pressure loss in tube bank condensers', *Ph.D. Thesis* 1973, Glasgow Univ., Scotland.
(3) CUNNINGHAM, J., and ALY, S. 'The effect of roughness on the pressure drop and shear stress round cylinders in cross flow', *Proc. 6th Int. Symp. Fresh Water from the Sea*, 1978, **1**, 137–144.
(4) MACVEAN, D., and ALY, S. 'A servo-force balance instrument for the direct measurement of wall shear stress on circular cylinders', *J. Phys. E. Sci. Instrum.* 1978, **11**, 1048–105.
(5) KESTIN, J., and WOOD, R. 'The influence of turbulence on mass transfer from cylinders', *J. Heat Transfer* 1971, 312–327.
(6) PEARCE, H. R. 'Noise and vibration in heat exchangers', *Ph.D. Thesis* 1973, Oxford, England.
(7) DEPOOTER, K., BRUNDRETT, E., and STRONG, A. B. 'Direct measurement of wall shear stress with mass transfer in a low speed boundary layer', *J. Fluids Eng.*, 1977, 580–584.
(8) HOERNER, S. *Aerodynamic Drag* 1951, (Ottenbein Press, Dayton, Ohio, USA.)
(9) ACHENBACH, E. 'Investigations on the flow through a staggered tube bundle at Reynolds numbers up to $Re - 10^7$', *Wärme- und Stoffübertragung* 1969, **2**, 47–52.
(10) ALLEN, H., and VINCENTI, W. 'Wall interference in a two dimensional flow wind tunnel, with consideration of the effect of compressibility', *Nat. Adv. Comm. Aero. Wash.*, Rep. 782, 1944.
(11) STASJULJAWITSCHIUS, K., *et al.* 'Heat transfer and fluid dynamics of staggered tube bundles with a transverse flow at $Re > 10^5$', *J. Eng. Physics*, 1964, **7(11)**, 10–15.
(12) ACHENBACH, E. 'Influence of surface roughness on the flow through a staggered tube bank', *Wärm- und Stoffübertragung* 1971, **4**, 120–126.
(13) JAKOB, M. 'Contribution to discussion on heat transfer and flow resistance in cross-flow of gases over tube banks', *Trans. A.S.M.E.* 1938, **59**, 384–386.
(14) GRIMISSON, E. D. 'Correlation and utilisation of new data on flow resistance and heat transfer for cross flow of gases over tube banks', *Trans. A.S.M.E.* 1937, **59(7)**, 583–594.
(15) ZUKAUSKAS, A. 'Heat transfer of banks of tubes in cross-flow at high Reynolds numbers', 1972, *Int. Centre for heat and mass transfer, Int. Seminar* Trogir, Yugoslavia, Session C.
(16) PANKHURST, R., and THWAITES, B. 'Experiments on the flow past a porous circular cylinder fitted with a Thwaites flap', *Aero. Res. Coun. R & M No. 2787*, 1950.
(17) SCHWABE, M. 'Pressure distribution in non-uniform two-dimensional flow', 1943, *Nat. Adv. Comm. Wash., Tech. Memo. No. 1039.*